A Platinum Open Access Journal for Organic Chemistry

Paper

Free to Authors and Readers | DOAJ Seal | *Arkivoc* **2025** (2) 202612565

Green synthesis of octahydroquinazolinone and hexahydroquinazolinone derivatives in aqueous medium catalyzed by nano bismuth oxide under mild conditions

Sanjog G. Mumbaikar and Vishvanath D. Patil*

Organic Chemistry Research Laboratory, Department Of Chemistry, C. K. Thakur A.C.S. College New Panvel, Raigad, Maharashtra, India
Email: vishvanathpatil148@gmail.com

This article is dedicated to Professor Rajender S. Varma in recognition of his outstanding contributions to green chemistry and sustainable synthetic methodologies

Received 02-15-2026 **Accepted** 08-23-2026 **Published online** 09-06-2026

Abstract

Green synthesis of octahydroquinazolinone and hexahydroquinazolinone derivatives was achieved using nano-bismuth oxide (Bi_2O_3) as an efficient and environmentally benign catalyst via a multicomponent reaction strategy. A Biginelli-type one-pot condensation of aldehydes, dimedone, and urea was carried out in water as a green solvent under mild reaction conditions. The protocol afforded the desired octahydroquinazolinone and hexahydroquinazolinone derivatives in high yields with a simple work-up procedure. The nano-Bi_2O_3 catalyst was readily separated and reused for successive cycles without significant loss of catalytic activity, demonstrating its potential as a sustainable and practical catalytic system for heterocyclic synthesis.

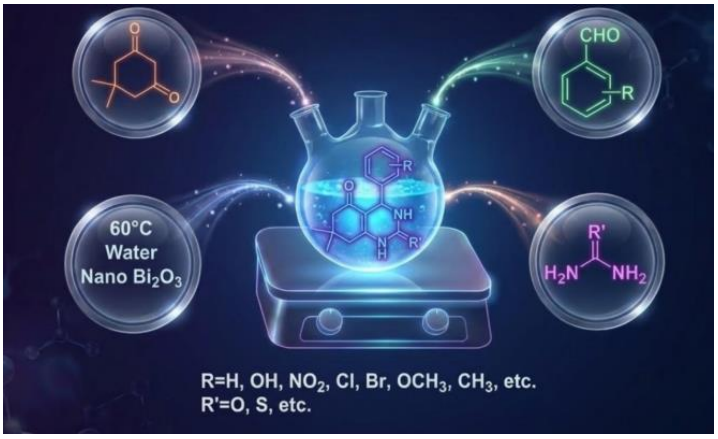

Keywords: Dimedone, nano catalyst, bismuth oxide, green synthesis, green solvent, recyclable catalyst

Introduction

Multicomponent reactions (MCRs) have emerged as one of the most efficient and sustainable synthetic strategies in modern organic chemistry because they enable the construction of complex molecular architectures from simple starting materials in a single operation. Such transformations offer several advantages, including high atom economy, operational simplicity, reduced waste generation, and shorter reaction times.[1–3] Owing to these benefits, MCRs have become powerful tools for the synthesis of biologically important heterocyclic compounds and pharmaceutical intermediates.[4]

Among the numerous MCR-based transformations, the Biginelli reaction has attracted considerable attention as a straightforward and efficient method for the synthesis of nitrogen-containing heterocyclic frameworks. The condensation of an aldehyde, urea (or thiourea), and an active methylene compound provides rapid access to structurally diverse heterocycles with significant biological and medicinal importance. Consequently, considerable efforts have been devoted to the development of efficient and environmentally benign catalytic systems for Biginelli-type reactions.

Octahydroquinazolinone and hexahydroquinazolinone derivatives represent an important class of fused nitrogen-containing heterocycles that exhibit a broad spectrum of biological activities, including antioxidant,[5] antitumor, antifungal, antibacterial and antitubercular,[6] analgesic, sedative and tranquilizing,[7] anticonvulsant,[8] antimicrobial and anesthetic,[9] anticancer,[10] antihypertensive,[11] anti-inflammatory,[12] diuretic,[13] and muscle-relaxant properties.[14] Because of these diverse pharmacological activities, the development of efficient synthetic methods for their preparation remains an active area of research.

Several catalytic protocols have been reported for the synthesis of octahydroquinazolinone derivatives. Catalysts such as trimethylsilyl chloride,[15] concentrated sulfuric acid,[16] Nafion-H,[17] NH4VO3,[18] and various Lewis acids and heterogeneous catalytic systems[19–28] have been successfully employed. Although these methods often provide satisfactory yields, many suffer from disadvantages such as harsh reaction conditions, prolonged reaction times, the use of hazardous solvents, complicated work-up procedures, non-recyclable catalysts, and environmental concerns.

To overcome these limitations, nanocatalysts have emerged as attractive alternatives because of their high surface area, enhanced catalytic activity, and ease of recovery and reuse.[2,26] In particular, bismuth oxide-based materials have gained considerable attention as environmentally friendly catalysts owing to their low toxicity, low cost, thermal stability, and excellent catalytic performance. Recent studies have demonstrated that Bi2O3-containing nanocomposites and Bi2O3-supported catalysts efficiently promote Biginelli-type reactions for the synthesis of dihydropyrimidinone derivatives under mild and solvent-free conditions.[29,30] These findings highlight the potential of bismuth oxide-based catalysts as sustainable alternatives to conventional catalytic systems.

Despite these advances, reports describing the use of nano-Bi2O3 as a catalyst for the synthesis of octahydroquinazolinone and hexahydroquinazolinone derivatives in aqueous medium remain limited. Therefore, the development of a simple, efficient, and environmentally benign protocol employing a recyclable nano-Bi2O3 catalyst under green reaction conditions is still highly desirable.

In view of the above considerations, we herein report an efficient one-pot synthesis of octahydroquinazolinone and hexahydroquinazolinone derivatives using nano-bismuth oxide (Bi_2O_3) as a recyclable catalyst in water. The methodology offers several advantages, including high yields, short reaction times, operational simplicity, catalyst recyclability, and the use of water as an environmentally benign solvent.

Results and Discussion

To evaluate and establish the most efficient catalytic framework for the synthesis of octahydroquinazolinone and hexahydroquinazolinone derivatives, a comparative study was conducted using various catalytic systems. A model multicomponent reaction was performed utilizing dimedone (1.0 mmol), benzaldehyde (1.0 mmol), and urea (1.0 mmol) in water (5 mL) at a baseline temperature of 60 °C (in water bath) (Table 1). The optimization studies were strategically initiated at a baseline temperature of 60 °C to provide the necessary thermal activation energy required for the initial Knoevenagel condensation step, which is often the rate-determining phase of this multicomponent sequence. Furthermore, this temperature was selected to enhance the solubility and mass transfer of the solid organic substrates dimedone, aromatic aldehydes, and urea within the aqueous phase, ensuring a more efficient interaction at the heterogeneous nano Bi_2O_3 catalyst interface. Among the various catalysts investigated, the nano Bi_2O_3 catalyst exhibited the most prominent catalytic activity, affording near-quantitative conversion within a significantly compressed timeframe (Table 1, entries 8–10).

Table 1. Synthesis of octahydroquinazolinone and hexahydroquinazolinone by reaction of dimedone, benzaldehyde and urea in the presence of different metal salt catalysts with H_2O solvent at 60 °C

Entry	Catalyst	Amount [mmol (mg)]	Time (min)	Product yield[a] (%)
1	$ZnFe_2O_4$	-	120	94
2	$CuCl_2$	0.2 (13)	180	78
3	CuO	0.2 (80)	180	20
4	Cu_2O_3	0.2 (11)	180	15
5	SiO_2	0.2 (6)	180	10
6	CaO	0.2 (6)	180	10
7	$Cu(BF_4)$ / SiO_2	0.1 (30)	30	96
8	Nano Bi_2O_3	0.1 (46)	15-20	98
9	NanoBi_2O_3	0.2 (93)	15-20	98
10	NanoBi_2O_3	0.3 (138)	15-20	98

[a]Isolated yield.

A critical analysis of the optimization profiles presented in Table 1 outlines the essential role of the nano-catalyst synthesized. While alternative metal oxides and supported catalysts required extended reaction periods and provided lower to moderate conversions (Table-1, Entries 2–6), the nano Bi_2O_3 matrix demonstrated superior kinetic acceleration. The optimization parameters revealed that a catalytic loading of 0.1 mmol of nano Bi_2O_3 was sufficient to deliver an excellent isolated yield of 98% within a rapid reaction latency of 15-20 minutes (Table 1, Entry 8). Intriguingly, increasing the catalyst loading further to 0.2 mmol or 0.3 mmol (Table 1, Entries 9 and 10) resulted in identical yields (98%) without shortening the reaction time.

Consequently, 0.1 mmol was determined to be the optimal catalytic concentration. Choosing this lower loading minimizes catalyst consumption and aligns with the green chemistry by optimizing atom economy and process cost-effectiveness while preventing unnecessary catalyst waste.

Table 2. Reactions of dimedone with benzaldehyde and urea under various conditions

Entry	Solvent	Nano Bi_2O_3 (mmol)	Time (min.)	Temp (°C)	Yield[a] (%)
1	Neat	-	200	80	10
2	CH_3CN	0.1	100	45	70
3	CH_2Cl_2	0.1	50	40	75
4	EtOH	0.1	50	70	78
5	EtOAc	0.1	100	60	70
6	DMF	0.1	60	80	85
7	H_2O	0.1	30	25	90
8	H_2O	0.01	30	60	75
9	H_2O	0.05	30	60	85
10	H_2O	0.10	15-20	60	98
11	H_2O	0.10	15-20	Reflux	98

[a]Isolated yield of the corresponding octahydroquinazolinone and hexahydroquinazolinone derivatives.

The experimental profiles summarized in Table 2 clearly indicate that the choice of solvent drastically impacts both the reaction kinetics and overall product yields. Conducting the transformation under solvent-free ("neat") conditions in the absence of the catalyst led to negligible product formation (Table 2, Entry 1, 10%), confirming that thermal activation alone is insufficient to drive this multi-component pathway efficiently.

When conventional organic solvents such as acetonitrile, dichloromethane, ethanol, ethyl acetate, and dimethylformamide were employed in the presence of 0.1 mmol of the nano Bi_2O_3 catalyst, only moderate to good yields (70–85%) were obtained alongside prolonged reaction times ranging from 50 to 100 minutes (Table 2, Entries 2–6).

In sharp contrast, utilizing water as the reaction medium provided a profound catalytic acceleration. Even at room temperature (25 °C), water delivered an impressive 90% isolated yield within 30 minutes (Table 2, Entry 7). This dramatic enhancement can be attributed to the unique "on-water" catalytic effect, where strong intermolecular hydrogen bonding at the aqueous interface stabilizes the polar transition states of the multi-component intermediate steps, thereby lowering the overall activation energy.

The reaction profile within the aqueous phase, the catalyst loading and thermal boundaries were systematically varied: Reducing the catalyst concentration to 0.01 mmol or 0.05 mmol at 60 °C resulted in diminished yields of 75% and 85%, respectively, despite doubling the reaction time to 30 minutes (Entries 8 and 9). Elevating the catalyst loading to the optimized 0.10 mmol at 60 °C successfully compressed the reaction latency to just 15-20 minutes, affording a near-quantitative isolated yield of 98% (Table 2, Entry 10). Increasing the temperature further to reflux conditions (Table 2, Entry 11) maintained the same high yield (98% in 15-20 min) but offered no kinetic advantage over operating at 60 °C.

Consequently, the reaction conditions optimized in Table-2, Entry 10 (0.10 mmol nano Bi_2O_3 in H_2O at 60 °C for 15-20 minutes) were selected as the standard protocol for investigating the subsequent substrate scope due to their superior efficiency, lower energy consumption, and strict alignment with green chemistry principles.

Table 3. Comparison of the present nano-Bi_2O_3 catalyzed protocol with previously reported methods for the synthesis of octahydroquinazolinone and hexahydroquinazolinone derivatives

Entry	Catalyst	Catalyst loading	Solvent	Temperature (°C)	Time (min)	Yield (%)	Advantages / Disadvantages	Reference No.
1	Conc. H_2SO_4	Stoichiometric	Solvent Free	Reflux	120	85	Corrosive catalyst, difficult handling	16
2	Nafion-H	10 mol%	Solvent Free	80	90	88	Expensive catalyst	17
3	NH_4VO_3	10 mol%	Ethanol	Reflux	75	90	Longer reaction time	18
4	Lewis acid catalyst	10 mol%	Organic solvent	Reflux	60	92	Use of organic solvents	19– 24
5	Bi_2O_3/ ZrO_2	10 mol%	Solvent free	80 °C	45	92	Reusable catalyst	30
6	Nano Bi_2O_3 (Present work)	10 mol%	Water	60 °C	15-20	98	Green solvent, high yield, short reaction time, recyclable catalyst	This work

Table 3 presents a comparative evaluation of the present nano-Bi2O3-catalyzed protocol with previously reported methods for the synthesis of octahydroquinazolinone and hexahydroquinazolinone derivatives. The comparison clearly demonstrates that the current methodology affords excellent product yields within shorter reaction times under relatively mild reaction conditions. Moreover, the use of water as a green solvent, together with the low catalyst loading and recyclability of nano-Bi2O3, makes the present protocol operationally simple, cost-effective, and environmentally benign compared with previously reported procedures.

To synthesize a wider set of octahydroquinazolinone and hexahydroquinazolinone derivatives, various aldehydes were subjected to the optimized reaction conditions (Scheme 1), and the results are summarized in Table 4. With the optimized reaction parameters firmly established (0.10mmol nano Bi_2O_3, H_2O as the green solvent at 60 °C), we subsequently explored the generality and versatility of this multi-component protocol. A wide array of structurally diverse aromatic aldehydes was reacted with dimedone and urea/thiourea equivalents to construct a broad library of functionalized octahydroquinazolinone and hexahydroquinazolinone derivatives (Table 4, Entry 1 to 20).

The multi-component condensations proceeded smoothly and efficiently, generating the target heterocyclic molecules in excellent isolated yields (90–98%) within highly compressed reaction timeframes (15–30min) without the formation of any detectable side products or complex mixtures. The remarkable operational simplicity and the absence of competitive side reactions underscore the high selectivity and robust efficiency of this green synthetic protocol.

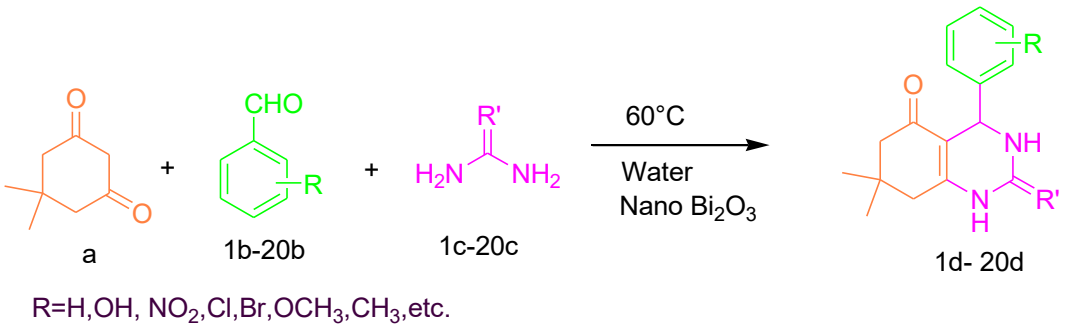

Scheme 1. Synthesis of octahydroquinazolinone and hexahydroquinazolinone derivatives.

Table 4. Synthesis of Octahydroquinazolinone and Hexahydroquinazolinone derivatives using dimedone and various aldehydes, urea equivalents and Nano Bi_2O_3

Entry	Aldehyde (b)	Substituted Urea (c)	Product (d)	Time (min.)	Mp ˚C (by Lit.)	Yield[b] (%)
1	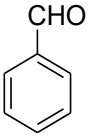	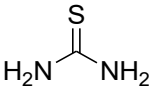	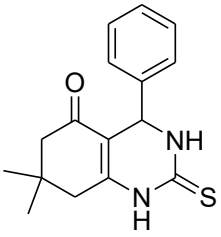 (1d)	15	283-285 (285-286)[1]	98
2	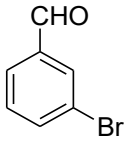	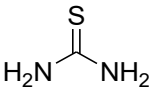	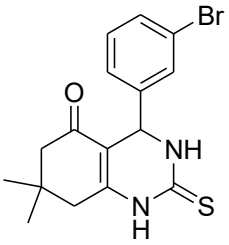 (2d)	20	262-264 (263-264)[27]	96
3	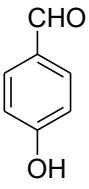	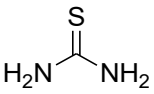	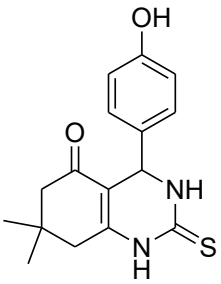 (3d)	20	275-278 (274-276)[2]	90

Table 4. Continued

Entry	Aldehyde (b)	Substituted Urea (c)	Product (d)	Time (min.)	Mp ˚C (by Lit.)	Yield[b] (%)
4	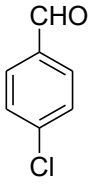	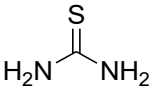	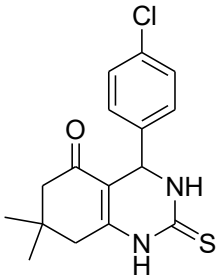 (4d)	20	272-275 (274-276)[2]	92
5	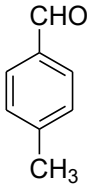	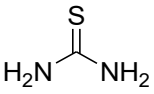	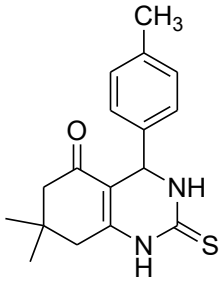 (5d)	30	278-280 (280-282)[22]	90
6	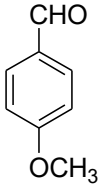	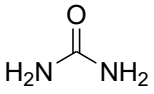	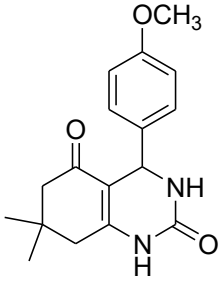 (6d)	20	273-275 (272-274)[22]	93
7	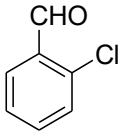	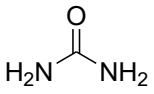	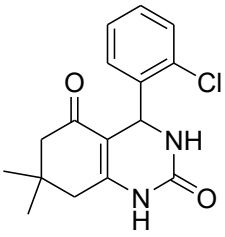 (7d)	15	270-272 (271-273)[22]	96
8	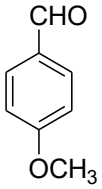	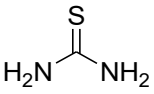	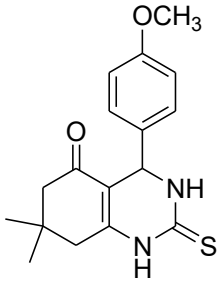 (8d)	30	270-272 (268-270)[22]	90

Table 4. Continued

Entry	Aldehyde (b)	Substituted Urea (c)	Product (d)	Time (min.)	Mp ˚C (by Lit.)	Yield[b] (%)
9	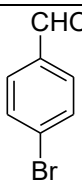	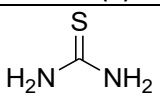	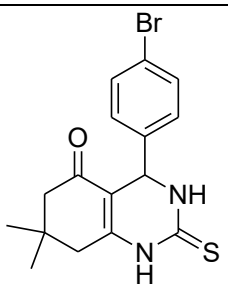 (9d)	20	283-285 (285-286)[15]	92
10	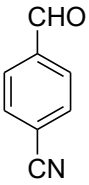	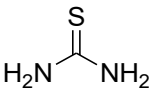	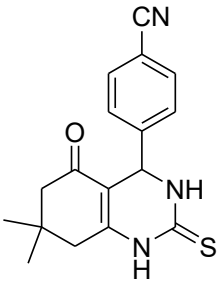 (10d)	25	269-271 (269-271)[2]	97
11	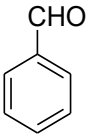	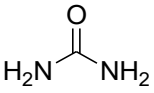	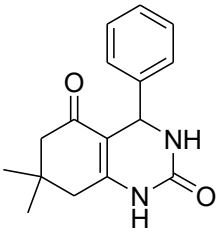 (11d)	15	291-294 (292-295)[15]	96
12	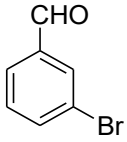	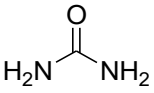	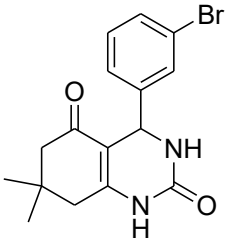 (12d)	20	264-266 (265-267)[22]	94
13	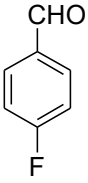	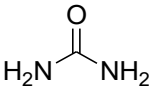	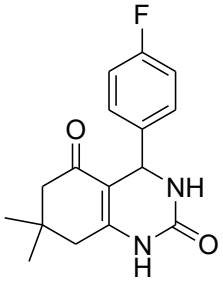 (13d)	20	301-304 (301-303)[27]	96

Table 4. Continued

Entry	Aldehyde (b)	Substituted Urea (c)	Product (d)	Time (min.)	Mp ˚C (by Lit.)	Yield[b] (%)
14	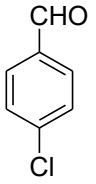	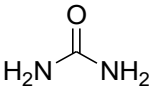	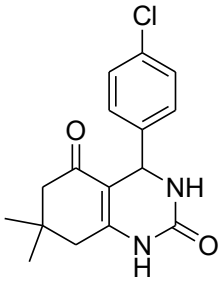 (14d)	20	315-317 (>300)[15]	92
15	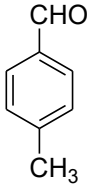	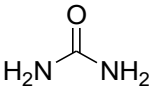	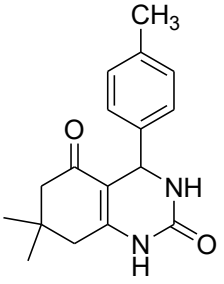 (15d)	30	272-276 (273-275)[15]	90
16	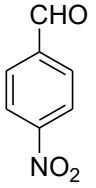	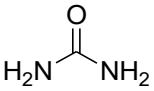	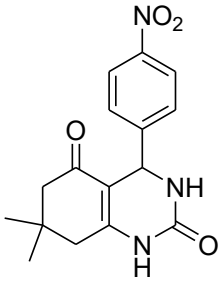 (16d)	15	302-304 (304-305)[16]	98
17	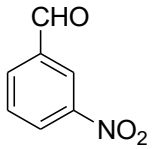	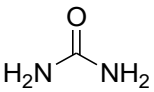	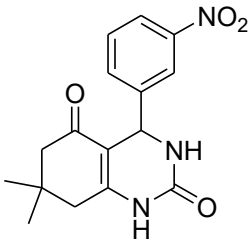 (17d)	15	297-300 (299-300)[17]	98
18	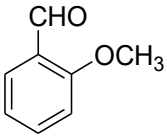	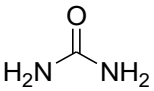	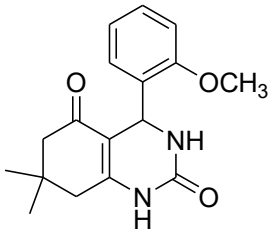 (18d)	30	200-204 (197-199)[22]	90

Table 4. Continued

Entry	Aldehyde (b)	Substituted Urea (c)	Product (d)	Time (min.)	Mp ˚C (by Lit.)	Yield[b] (%)
19	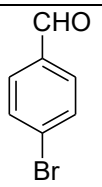	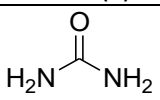	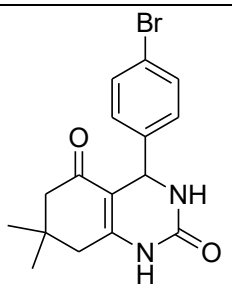 (19d)	20	304-307 (>300)[15]	92
20	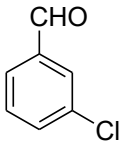	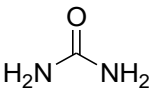	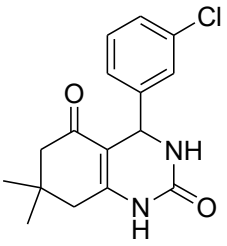 (20d)	25	292-294 (290-292)[22]	90

[a]Selected products were identified by their IR and ^{1}H NMR spectra, LC-MS.
[b]Isolated yields after column chromatography.

An evaluation of the electronic and steric profiles of the aromatic aldehyde substituents demonstrated a clear correlation with reaction efficiency. Aromatic aldehydes possessing strong electron-withdrawing groups (EWGs) such as NO_2 exhibited significantly enhanced electrophilic reactivity at the carbonyl carbon. This strong induction effect facilitated rapid attack by the nucleophilic components, thereby providing excellent yields in shorter reaction times, as demonstrated by the nitro-substituted variants (Table 4, entries 16 and 17). Halogenated substituents Cl, Br, and F (Table 4, entries 2, 4, 7, 9, 12, 13, 14, 19 and 20) also participated effectively, produced expected product profiles in a rapid manner due to their weak electron-withdrawing nature.

Conversely, aromatic aldehydes bearing electron-donating groups (EDGs) such as methoxy (-OCH_3) or methyl (CH_3) functionalities displayed slightly lower overall reactivity. The presence of these electron-releasing groups increases the electron density on the formyl carbon atom, which reduces its inherent electrophilicity. Consequently, these transformations required moderately prolonged reaction times (25–30min) to achieve high conversion metrics (Table 4, entries 5, 6, 8, 15, and 18).

Importantly, despite these localized electronic variances, the nano Bi_2O_3 catalytic system demonstrated exceptional functional group tolerance. Both urea and thiourea equivalents were compatible with the workflow, delivering high yields of oxygenated and sulfur-containing derivatives respectively, confirming the broad applicability of this aqueous framework.

Study of reusability of Nano Bi_2O_3:-

Economic viability and recyclability are critical parameters that define the efficiency of a heterogeneous catalyst in green chemical synthesis. Throughout the multi-component synthesis of the octahydroquinazolinone/ hexahydroquinazolinone derivatives, the nano Bi_2O_3 catalyst exhibited distinct

heterogeneous characteristics, remaining insoluble in the aqueous reaction mixture. This allowed for its facile physical separation and recovery via simple filtration or centrifugation.

To evaluate its operational durability, the recovered catalyst was thoroughly washed with distilled water followed by ethanol to remove any adhering organic residues, dried under vacuum, and re-subjected to fresh model reaction components under optimized conditions. As compiled in Table 5, the nano Bi_2O_3 matrix demonstrated outstanding chemical stability and robust efficiency, maintaining its catalytic integrity over five consecutive cycles with only a negligible decline in overall product yield.

Table 5. Reusability study of nano Bi_2O_3 catalyst for the synthesis of octahydroquinazolinone and hexahydroquinazolinone derivatives

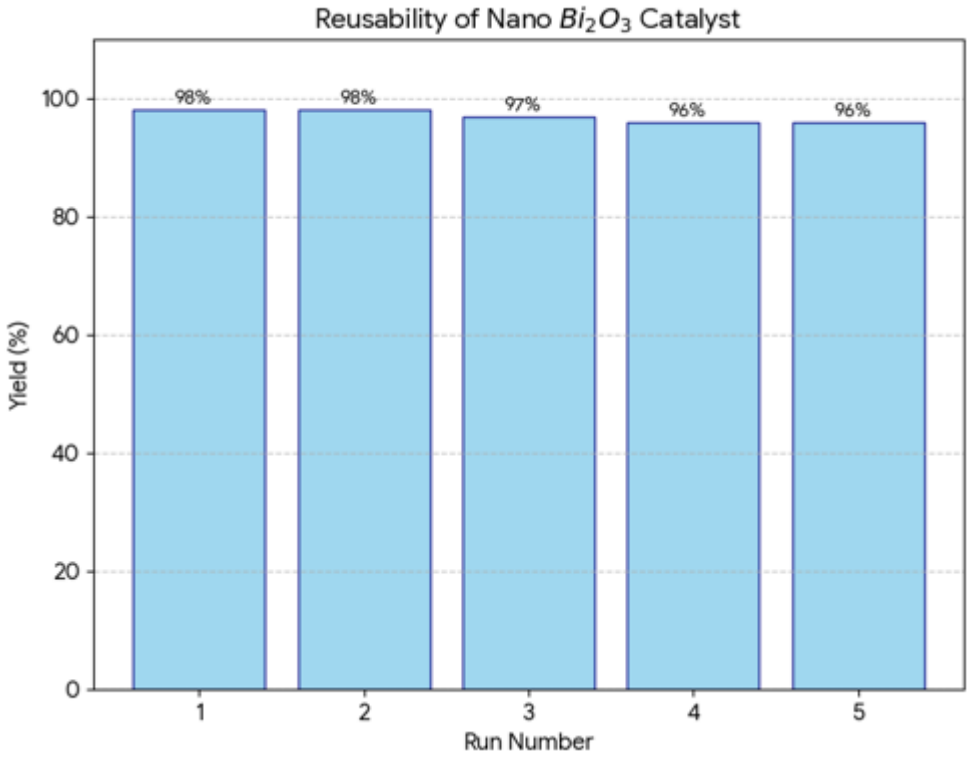

*Reaction conditions; Dimedone (1.0 mmol), benzaldehyde (1.0 mmol), substituted urea (1.0 mmol), 0.1mmol of Nano Bi_2O_3 in water (4 mmol) at 60°C. [c]Isolated Yield.

Conclusions

The utility of nano Bi_2O_3 as a heterogeneous and reusable catalyst in the synthesis of octahydroquinazolinone and hexahydroquinazolinone derivatives demonstrates significant potential for broader applications in sustainable organic synthesis. Beyond the current scaffold, this methodology provides a foundation for exploring the catalytic efficiency of bismuth-based nanoparticles in other multi-component reactions (MCRs) to access diverse pharmacologically active heterocycles. Furthermore, the high surface-area to volume ratio and low toxicity of bismuth, often regarded as a 'green' heavy metal, should encourage future research into immobilized catalytic systems for use in continuous flow chemistry. Such advancements would facilitate

industrial scalability and minimize environmental impact. Subsequent studies focusing on the synergistic effects of doping nano Bi_2O_3 with other transition metals could further optimize reaction times and yields for electronically deactivated or sterically hindered substrates, thereby expanding the strategic toolkit for pharmaceutical intermediate production.

Experimental Section

General. The required compounds were all analytical grade (AR) and didn't need to be further purifications. The synthetic octahydroquinazolinone and hexahydroquinazolinone derivatives ^{1}H NMR spectra were recorded using a 400 MHz DELTA NMR spectrometer. The values of each chemical shift were expressed in terms of δ and as parts per million, with tetramethylsilane (TMS, δ=0) serving as an internal standard. A Bruker FT-IR spectrometer was used to record each infrared spectrum. Each synthetic octahydroquinazolinone and hexahydroquinazolinone derivative was identified by comparing its melting point data with trustworthy information from the literature. Spectrum data for a variety of octahydroquinazolinone and hexahydroquinazolinone derivatives were obtained.

General experimental procedure. Preparation of octahydroquinazolinone and hexahydroquinazolinone derivatives: a 50 mL round-bottom flask equipped with a magnetic stirrer with dimedone (1.0 mmol, 1 equiv), benzaldehyde (1.0 mmol, 1 equiv), thiourea (1.0 mmol, 1 equiv), and Bi_2O_3 nano-catalyst (0.1 mmol). The reaction mixture was stirred at 60°C (water bath) in the presence of 5 mL of water. The progress of the reaction was monitored by thin-layer chromatography (TLC; Pet Ether/ethyl acetate in 7:3). Upon completion of the reaction, the mixture was cooled to room temperature and extracted with ethyl acetate (3 × 10 mL). The heterogeneous nano-Bi2O3 catalyst was separated by filtration and washed with ethyl acetate for reuse. The combined organic extracts were transferred to a separating funnel, washed with brine (15 mL), and dried over anhydrous sodium sulfate. Removal of the solvent under reduced pressure afforded the crude product.
Final purification of the compounds was achieved via column chromatography on silica gel (60–120 mesh) using an appropriate gradient of Pet Ether and ethyl acetate to form the octahydroquinazolinone and hexahydroquinazolinone product. and characterized using IR, both ^{1}H and ^{13}C NMR spectroscopy and LC-MS.
Preparation of nano Bi_2O_3. Bismuth nitrate pentahydrate (0.48 g) was employed as the metal ion precursor for the synthesis of nano bismuth oxide. A stoichiometric amount of glycine (0.075 g) and L-ascorbic acid (0.017 g) were added to the reaction with a minimal volume of deionized water (5 mL) to facilitate dissolution. The resulting transparent solution was gradually heated on a hot plate at 80 °C to promote homogenization and gel formation. Upon further heating, the water content evaporated, and the gel began to combust, releasing brownish fumes for a brief period (2–3 seconds). This process yielded a yellowish powder, which was subsequently calcined in a muffle furnace at 600 °C for 4 hours to remove residual carbonaceous matter. The final product comprised fine Bi_2O_3 nanoparticles with a particle size distribution ranging between 8 nm and 16 nm (Figure 4).

Nanomaterial characterization

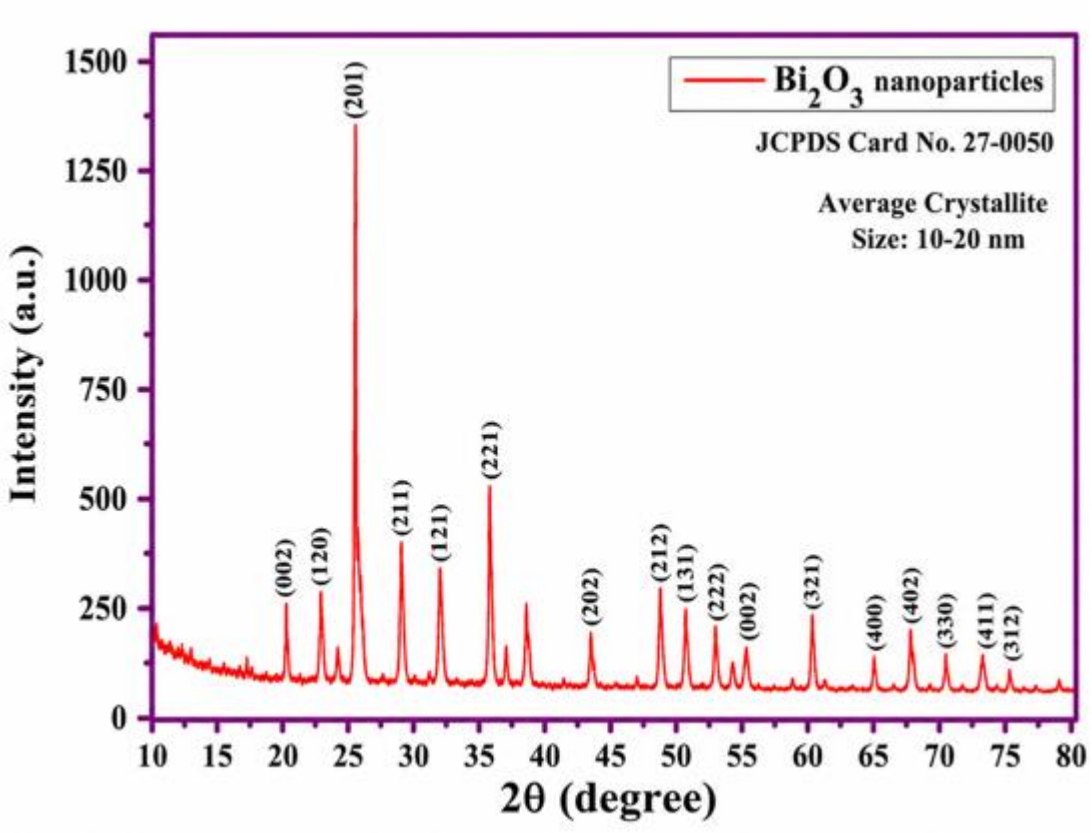

Figure 1. XRD pattern of Nano Bi_2O_3.

The XRD pattern of Bi_2O_3 nanoparticles (Figure 1) exhibits sharp and well-defined diffraction peaks, confirming the crystalline nature of the synthesized material. The prominent diffraction peak observed at 2θ ≈ 25.8° is indexed to the (201) plane, while other characteristic peaks located at ~20.3°, 23.1°, 29.4°, 32.0°, 35.8°, 43.5°, 48.8°, 50.7°, and 60.5° correspond to the (002), (120), (211), (121), (221), (202), (212), (131), and (321) planes, respectively. These diffraction peaks are in good agreement with the standard JCPDS data for Bi_2O_3 (Card No. 27-0050), confirming the formation of crystalline Bi_2O_3 nanoparticles. No additional impurity peaks were observed, indicating the high purity of the synthesized sample. The average crystallite size was estimated using the Scherrer equation, $D=K\lambda/\beta\cos\theta$ and was found to be in the range of 10–20 nm, confirming the nanocrystalline nature of Bi_2O_3 nanoparticles.

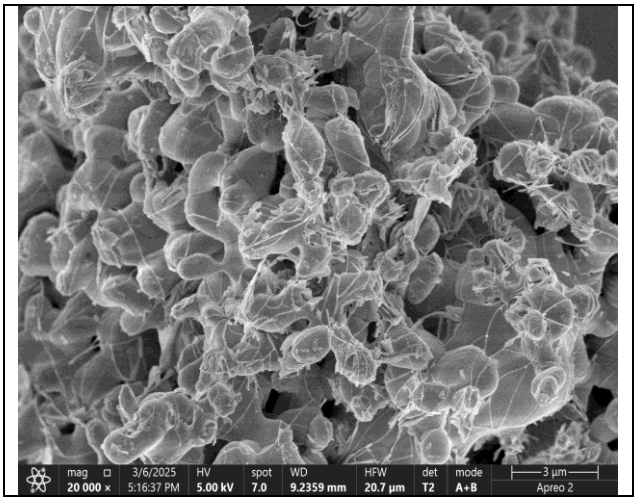

Figure 2. SEM Analysis of Nano Bi_2O_3.

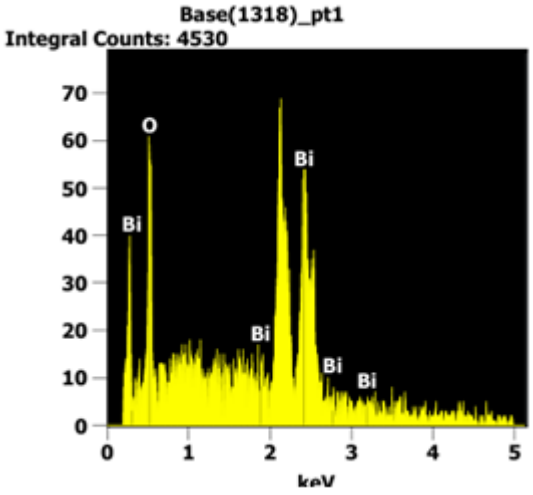

Figure 3. SEM EDX Analysis of Nano Bi_2O_3.

The surface morphology of Bi_2O_3 nanoparticles has been studied using FESEM and shown in (Figure 2). & it shows porous flower type morphology. The presence of Bismuth and Oxygen was observed by EDAX (Figure 3).

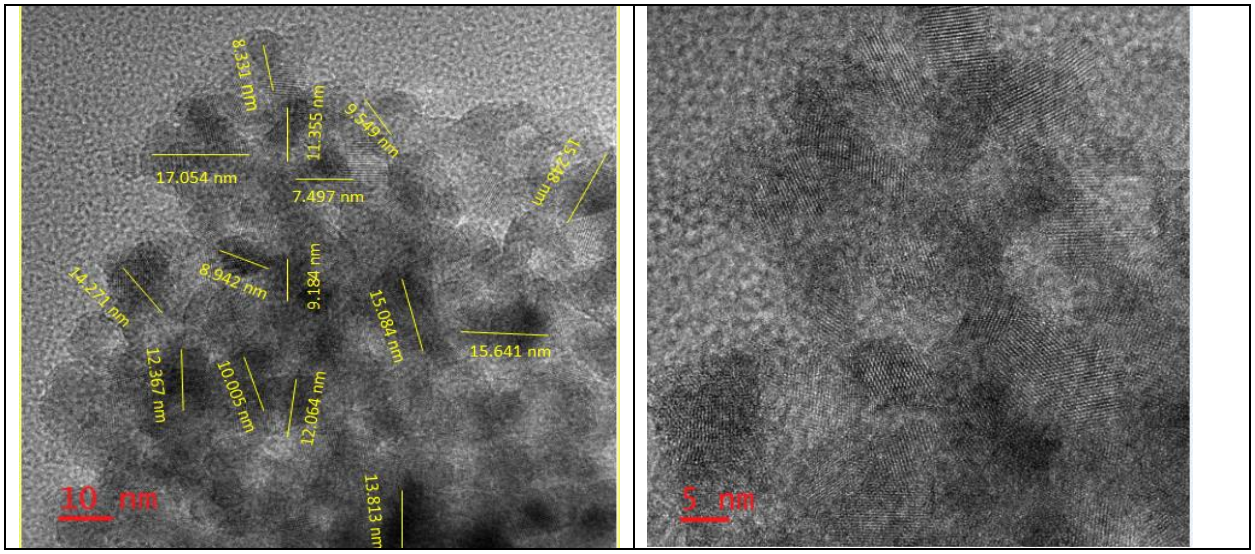

Figure 4. TEM analysis of Nano Bi_2O_3.

The size of the Bi_2O_3 nanoparticles was also determined using an HRTEM image, and it is found in the range of 8 to 16 nm. (Figure 4)

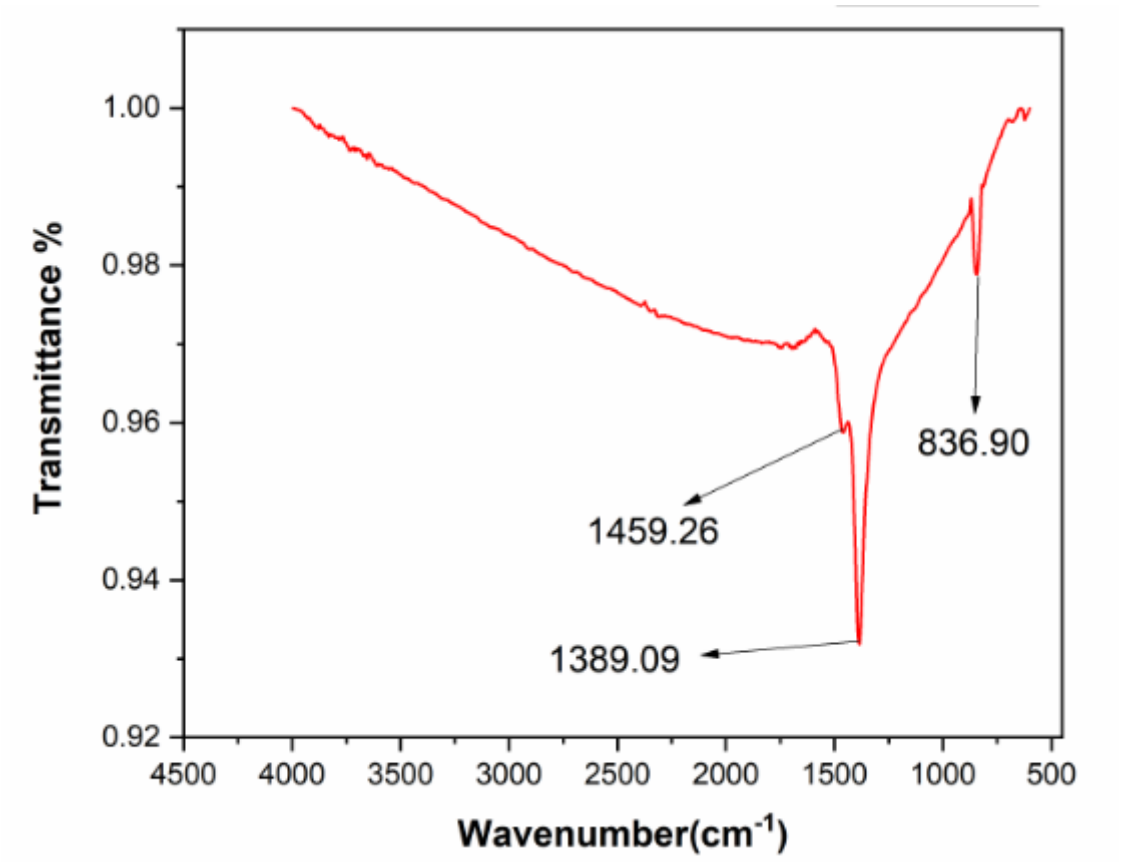

Figure 5. IR Analysis of Nano Bi_2O_3.

The functional groups and bonding interactions present in Bi_2O_3 nanoparticles were identified by analyzing the FTIR spectrum of the Bi_2O_3 nanoparticles (Figure 5) in the spectral range of 400–4000 cm-1. The strong band at

836.90 cm^{-1} is characteristic of metal–oxygen (M–O) stretching vibrations, which confirm the formation of Bi_2O_3 nanoparticles. The absorption band appearing at 1459.26cm^{-1} and the sharp vibrational peak centered at 1389.09 cm^{-1} correspond to the typical bending and stretching modes of oxy-carbonate species or surface-coordinated interstitial bonds formed during the nano-fabrication phase.

Acknowledgements

The authors would like to sincerely thank the Department of Chemistry at C.K. Thakur A.C.S. College in New Panvel, affiliated University of Mumbai, for their support and provision of the equipment required to complete this work.

Supplementary Material

Yields and characterization data for selected compounds are provided in the Supporting Information document.

References

1. Patil, V.D.; Salve, A.M.; Gharart, V.D.; Gawand, N. *Res. J. Chem. Environ.* **2021**, *25*, 83–88. https://doi.org/10.25303/258rjce8389
2. Rao, T.N.; Krishnarao, N.; Ahmed, F.; Alomar, S.Y.; Albalawi, F.; Mani, P.; Aljaafari, A.; Parvatamma, B.; Arshi, N.; Kumar, S. *Nanomaterials* **2023**, *13*, 2527. https://doi.org/10.3390/nano13182527
3. Lednicer, D.; Mitscher, L.A. *The Organic Chemistry of Drug Synthesis*; Wiley Interscience: New York, **1980**; Vol. 2, p. 361. https://doi.org/10.1002/9780470293058
4. Kershaw, S.; Stables, J.P.; Jatav, V.; Mishra, P. *Eur. J. Med. Chem.* **2008**, *43*, 135–141. https://doi.org/10.1016/j.ejmech.2007.03.011
5. Sayed, R.E.; Wasfy, A.F. *J. Chin. Chem. Soc.* **2005**, *52*, 129–135. https://doi.org/10.1002/jccs.200500019
6. Tyagi, M.; Pathak, U.S.; Rathod, R.S. *Indian J. Chem.* **1995**, *34B*, 617–623.
7. Thierry, B.A.; Jerome, G.; Charles, W.R. *Tetrahedron Lett.* **2020**, *41*, 1027–1030. https://doi.org/10.1016/S0040-4039(00)00115-0
8. Bahl, B.S.; Bahl, A. *Textbook of Organic Chemistry*; Chand and Company Ltd.: New Delhi, **1997**; Vol. 14, p. 735.
9. Guiry, P.J.; Connolly, D.J.; Cusack, D. *Tetrahedron* **2005**, *61*, 10153–10202. https://doi.org/10.1016/j.tet.2005.07.062
10. Feng, L.; Meng, Q.; Feng, Y. *Arkivoc* **2007**, *(i)*, 40–50. https://doi.org/10.3998/ark.5550190.0008.105
11. Meyyanathan, S. *ASEAN Rev. Biodivers. Environ. Conserv.* **1998**, *2*, 4–10.
12. Alexandra, P.B.; Thierry, B.; Corinne, F. *Catalysts* **2000**, *10*, 1–34.

https://doi.org/10.3390/catal10010001
13. Lidstrom, P.; Tierney, J.; Westman, J. *Tetrahedron* **2001**, *57*, 9225–9283. https://doi.org/10.1016/S0040-4020(01)00906-1
14. Lottie, B.; Thomas, H. *J. Chem. Res.* **2000**, *2*, 42–46. https://doi.org/10.1243/0309324001513711
15. Canevari, S.; Bantu, R.; Nagarapu, L. *Arkivoc* **2006**, *(xvi)*, 136–148. https://doi.org/10.3998/ark.5550190.0007.g14
16. Hassani, Z.; Islami, M.R.; Kalantari, M. *Bioorg. Med. Chem. Lett.* **2006**, *16*, 4479–4482. https://doi.org/10.1016/j.bmcl.2006.06.038
17. Lin, H.; Zhao, Q.; Xu, B.; Wang, X. *J. Mol. Catal. A: Chem.* **2007**, *268*, 1–2. https://doi.org/10.1016/j.molcata.2006.11.050
18. Niralwad, K.S.; Shingate, B.; Shingare, M.S. *Tetrahedron Lett.* **2010**, *51*, 3616–3619. https://doi.org/10.1016/j.tetlet.2010.05.009
19. Mobinikhaledi, A.; Foroughifar, N.; Khodaei, H. *Eur. J. Chem.* **2010**, *1*, 291–295. https://doi.org/10.5155/eurjchem.1.4.291-295.151
20. Kefayati, H.; Asghari, F.; Khanjanian, R. *J. Mol. Liq.* **2012**, *172*, 147–151. https://doi.org/10.1016/j.molliq.2012.05.011
21. Khurana, J.M.; Kumar, S. *Monatsh. Chem.* **2010**, *141*, 561–564. https://doi.org/10.1007/s00706-010-0288-1
22. Karami, S.; Karami, B.; Khodabakhshi, S. *J. Chin. Chem. Soc.* **2013**, *60*, 22–27. https://doi.org/10.1002/jccs.201200234
23. Pachpinde, A.M.; Langade, M.M. *Int. J. Res. Appl. Sci. Biotechnol.* **2019**, *6*, 23–26. https://doi.org/10.31033/ijrasb.6.3.4
24. Kumar, B.V.; Naik, H.S.B.; Girija, D. *J. Chem. Sci.* **2011**, *123*, 615–621. https://doi.org/10.1007/s12039-011-0131-x
25. Beletskaya, I.; Tyurin, V. *Molecules* **2010**, *15*, 4792–4814. https://doi.org/10.3390/molecules15074792
26. Hemalatha, K.; Madhumitha, G.; Kajbafvala, A.; Anupama, N.; Sompalle, R.; Roopan, S.M. *J. Nanomater.* **2013**, *2013*, 1–23. https://doi.org/10.1155/2013/419510
27. Mobinikhaledi, A.; Foroughifar, N.; Khodaei, H. *Eur. J. Chem.* **2010**, *1*, 291-293. https://doi.org/10.5155/eurjchem.1.4.291-293.150
28. Yarim, M.; Saraç, S.; Kiliç, F. S.; Erol, K. *Il Farmaco* **2003**, *58*, 17-24. https://doi.org/10.1016/S0014-827X(02)00007-4
29. Mirzazadeh, A.; Hakimyfard, A.; Tahmasebi, N.; Kafi-Ahmadi, L.; Khademinia, S. *J. Korean Ceram. Soc.* **2023**, *60*, 856–867. https://doi.org/10.1007/s43207-023-00309-w
30. Guguloth, V. C.; Gajula, R.; Basude, M.; Battu, S. *Int. J. Chem. Anal. Sci.* **2014**, *5*, 86-92. https://doi.org/10.1016/j.ijcas.2014.04.001